

Electrical properties of soda lime silica glass using electrolysis at 600°C between molten tin and lead electrodes

J. K. HIGGINS

Lathom Laboratories, Pilkington Brothers, Ormskirk, Lancashire, UK

Received 25 April 1971; revised MS received 1 August 1971.

The electrolysis of a soda lime silicate glass has been studied using liquid metal electrodes of lead and tin at 600°C and voltages up to 300 V in a N₂/10% H₂ atmosphere. The behaviour observed was dependent upon the applied voltage. At less than 2.5 V, the square of the current was inversely proportional to the electrolysis time but at higher voltages, up to 100 V, the current was inversely proportional to the time for periods up to 300 ms. At voltages greater than 100 V, the behaviour could not be expressed by a simple equation, the currents passing were high and finally, electrical breakdown occurred at 300 V.

It is proposed that in the range 2.5 to 100 V the glass behaves as a dielectric with charge separation in a thin surface layer. At higher voltages, near breakdown, the heat liberated at the surface is sufficient to disrupt the surface layer and then the conduction is governed by the electrical properties of the bulk glass.

Introduction

Early studies on the electrolysis of soda lime silicate glass were made separately by Warburg [1] and Tegetmeier [2] using liquid metal electrodes. At 500°C they found using mercury anodes either alone or with added Ca, Mg, Al, Zn, Bi, or Au, that the current fell rapidly on completing the circuit. If Na or Li were present in the alloy, however, these elements replaced the Na ions in the glass and the current remained fairly steady for long periods. It was decided to study the fast electrochemical changes occurring in the first type of system using high speed recording techniques. Lead was chosen initially as a suitable low melting anode material. Reactions at the cathode were not generally considered.

Experimental

The electrolysis cell is shown in Fig. 1. It consisted of a stainless steel crucible, internal diameter 2.25 cm, height 4 cm, supported on a

rod of the same material screwed into its base. This rod and the crucible itself formed the cathode; the anode was a similar rod dipping into the upper metal pool.

About 9 g of A.R. tin were placed in the crucible followed by a disc of soda lime silicate glass, 2 cm diameter, 0.4 cm thick. On top of this was an annulus of 'Purox' alumina, internal diameter 1.5 cm, wall thickness 2 mm, the edge in contact with the glass being ground flat. Approximately 6 g of A.R. lead shot were placed inside the annulus and it was found that when the metal was melted, it did not flow out but remained inside the annulus as a pool. Initially, however, experiments were confined to 600°C at which temperature the currents were easily measurable and the glass remained reasonably undistorted. The area of the lead in contact with the glass was 1.54 cm².

The glass used was commercially available float glass; its composition in wt.% is given in Table 1. Before electrolysis about 1 mm was ground off both faces of the sample before final

polishing with rouge to remove all possibility of surface contamination by the tin of the float bath.

The cell was placed in the heating chamber of the inert gas furnace, a Nichrome wound 'Purox' alumina tube of internal diameter 3 cm, length 67 cm, and the supporting rod electrodes were

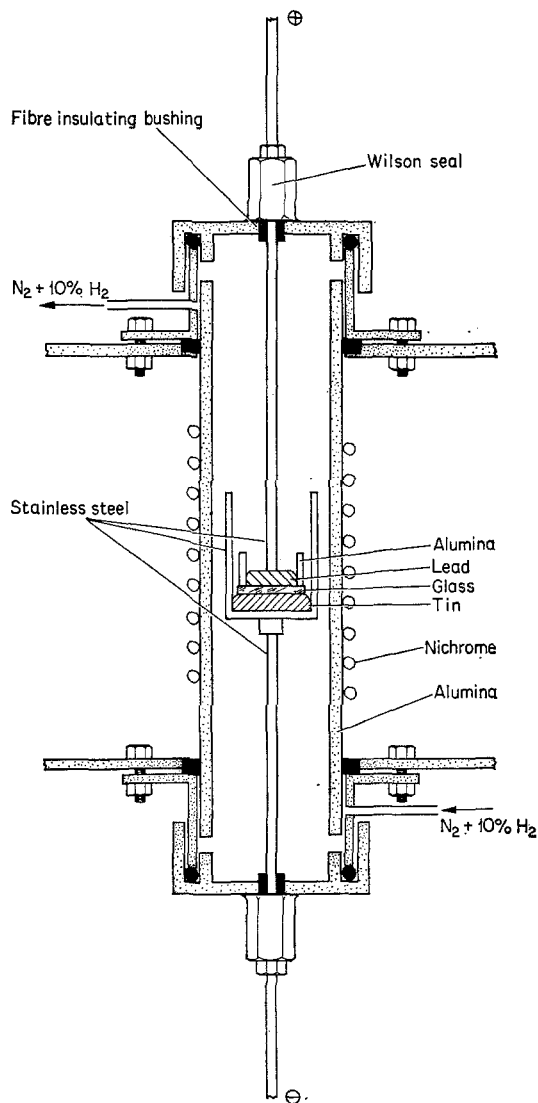


Fig. 1. Electrolysis cell.

insulated from the brass end-caps by fibre bushings as shown. The temperature was controlled to $\pm 0.5^\circ\text{C}$ by a Pt/13% Pt Rh thermocouple, an Ether proportional controller, type 1292 and a thyristor assembly, type 2635. Temperatures were recorded using a Leeds and Northrup Speedomax W Recorder.

The gas supply, a metered mixture of white spot N_2 and 10% H_2 , flowed at $100\text{ cm}^3/\text{min}$ through two separate 'Deoxo' units and Anhydron drying columns before passing through a needle valve into the furnace. On emerging via an oil bubbler, the oxygen and water vapour concentrations in the gas were measured using a Hersch meter and Beckmann electrolytic hygrometer. The values were <10 and <20 ppm respectively.

The electrical circuit is shown in Fig. 2. It

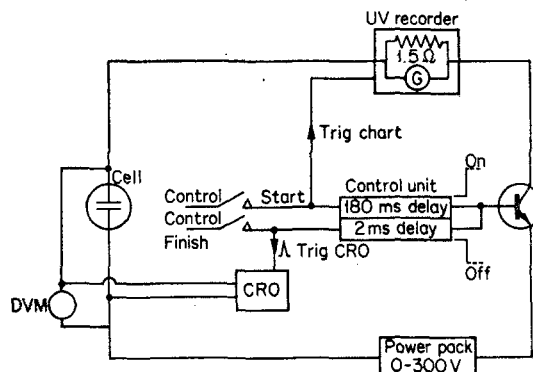


Fig. 2. Electrical circuit.

consisted essentially of a Trygon RS 320-1.2B power pack capable of supplying 1.2 A at 350 V with a load regulation of 0.01%. This was connected in series with the cell and an S.E. Laboratories U.V. Recorder, type SE 2005 with galvanometers of sensitivity 0.053, 0.0053 and 0.00083 mA/cm shunted across resistors of 1 to 5 Ω . A Measurement Research Control Unit completed the circuit through a Motorola, type MJ413752 power transistor.

In operation the power pack voltage was set and, on pressing the control start button, the

Table 1. Glass analysis (wt%).

Material	SiO_2	CaO	Fe_2O_3	Al_2O_3	MgO	Na_2O	K_2O
Concentration (%)	72.5	8.9	0.10	1.1	3.4	13.2	0.6

control unit switched on the power transistor 180 ms after it had started the recorder chart. This was necessary to allow the chart to attain a uniform speed before recording the I/t trace because most of the experiments were carried out at the high chart speed of 2 m s^{-1} . It was possible with the control unit to select ranges with full scale deflections of from 50 to 2,500 mA and calibration facilities were provided by accurate, wire wound resistors of tolerance $\pm 0.5\%$.

The voltage decay on breaking the circuit was followed using a Tektronix 564 storage oscilloscope with type 2A63 differential amplifier. On releasing the control start and pressing the control finish button, the control unit supplied a trigger pulse to the oscilloscope 2 ms before it switched out the power pack and enabled the start of the voltage drop to be located accurately.

A Bradley, type 160, digital voltmeter with 1 mV resolution was used to follow the decay for longer periods. Power pack voltages were measured with a Weston Model S 82 d.c. voltmeter and a.c. resistances and capacitances with a Marconi universal bridge, TF2700 at 1,000 Hz.

Results

In Fig. 3 a typical current time curve obtained at an applied voltage of 25 V is given. It consists of a branch AB in which the current rises rapidly to 137 mA in about 1 ms. This is followed by a fall of current along BC, the value at 300 ms being about 16 mA. A striking feature is the speed at which the process is finished; in most experiments the current usually becomes too small to measure accurately after 300 ms and most of the results quoted are for experiments of this duration.

The high peak value recorded at A is due to galvanometer overswing. This was 7% for the 0.053 mA/cm galvanometer used and a more correct value for the current at A is 127 mA. The slight ripple in the curve BC may be ascribed to galvanometer vibration.

The current at any point varies inversely with time; this is shown in Fig. 4. The graph may be represented by the equation:

$$(190t + 7)I = 1 \quad (1)$$

where I is in amperes and t is in seconds.

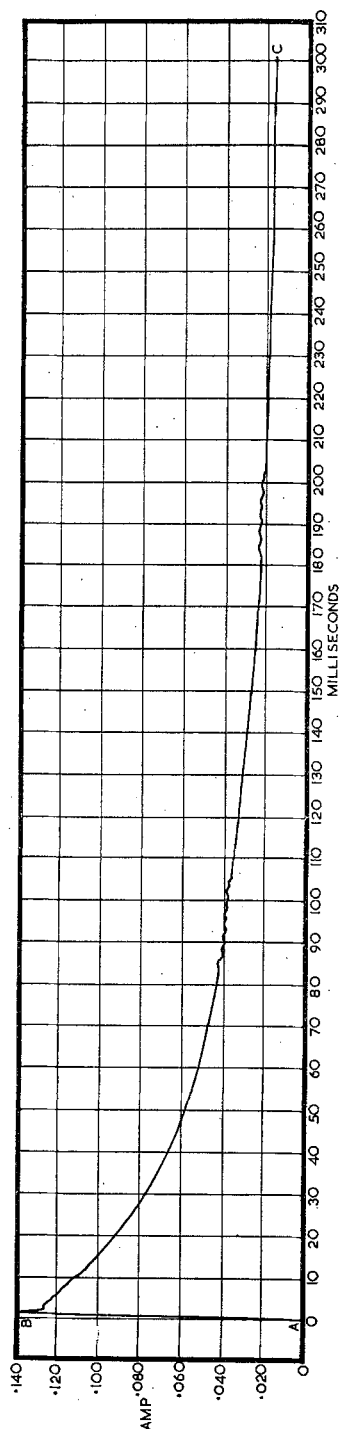


Fig. 3. Current-time trace at 25 V. Speed 2 m s^{-1}

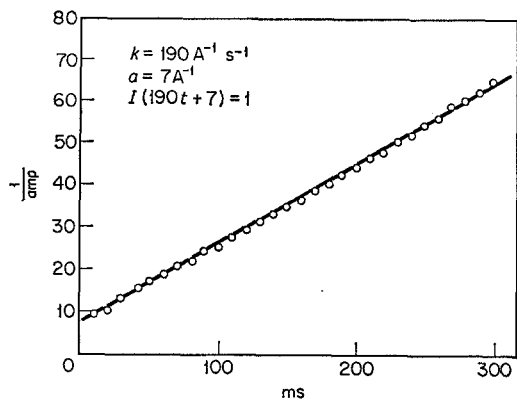


Fig. 4. Graph of current reciprocal against time at 25 V.

If the voltage is applied a second time the original behaviour is not exactly repeated. Fig. 5 shows a series of $1/I$ against t plots at 25 V obtained at hourly intervals. Although the graphs

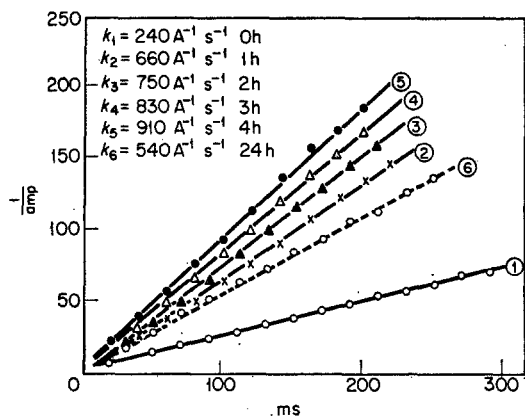


Fig. 5. Graph of current reciprocal against time at 25 V successive pulses.

are still linear the gradient increases with each successive electrolysis. If the system is left for longer periods, however, recovery is more nearly complete. Thus, the dotted curve (6) was obtained 24 hours and four treatments after (1) but it approaches this curve more closely than (2) which immediately succeeded it.

Similar experiments were carried out at voltages from 0.5 to 300 V. The results fell into three distinct categories depending upon the size of the applied voltage.

(1) At less than 2.5 V, the square of the current varied inversely with time according to the equations given in Table 2 and Fig. 6.

(2) From 2.5 to 100 V the behaviour was similar to that considered for 25 V and the current varied inversely with the time (Table 2). Successive treatments at the lower voltage in this range continued to give linear plots (Fig. 5) but at the

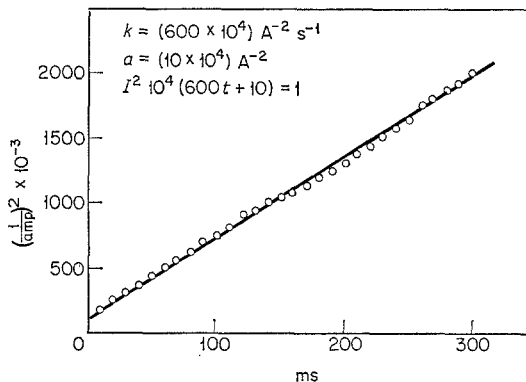


Fig. 6. Graph of (current reciprocal)² against time at 2.5 V.

Table 2. Current-time equations at 600°C.

Voltage	m	a	Equation ($mt + a$) $I = 1$	Resistance $t = 0$ (Ω)	Range (ms)
100	46	1.4	($46t + 1.4$) $I = 1$	197	0-450
75	51	2.6	($51t + 2.6$) $I = 1$	288	0-300
50	63	6.5	($63t + 6.5$) $I = 1$	325	0-350
25	190	7.0	($190t + 7$) $I = 1$	182	0-400
12	400	23	($400t + 23$) $I = 1$	315	0-300
5	1000	54	($1000t + 54$) $I = 1$	357	0-350
2.5	940	100	($940t + 100$) $I = 1$	250	0-350
1.0	610×10^4	10×10^4	$I^2 \cdot 10^4 (600t + 10) = 1$	314	0-300
0.5	850×10^5	8×10^5	$I^2 \cdot 10^5 (850t + 8) = 1$	450	0-300

I in amperes; t in seconds

higher voltages, while the first $1/I$ against t graph was linear, the second was usually curved. This is shown in Fig. 7 for 100 V.

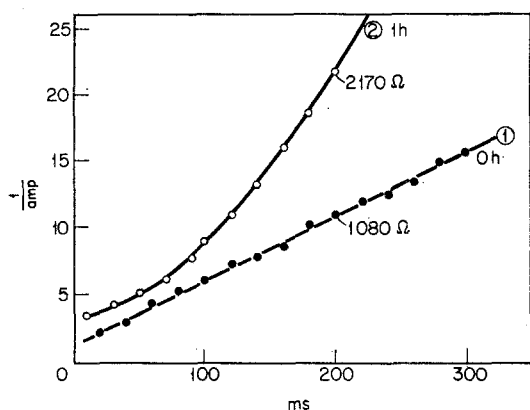


Fig. 7. Graph of current reciprocal against time at 100 V successive pulses.

(3) At voltages higher than 100 V the curves could not be expressed by a simple equation. The $1/I$ against t plots were not linear but curved upwards even for the first electrolysis (125 V). At 175 V the current started to rise again after about 45 ms (Fig. 8) and at 200 V and 250 V (Fig. 9) the currents did not fall appreciably at all after the initial surge but remained steady at 450 mA and 550 mA respectively. Finally, at 300 V, large current oscillations were observed (Fig. 10) and electrical breakdown occurred.

The resistance value corresponding to the steady currents observed at 200 V and 250 V was 450Ω and the resistances calculated from the high initial currents at the start of the I versus t curves at lower voltages are given in Table 2. They are of the same order as the a.c. bridge resistance of 270Ω measured on all samples before the start of the experiment. However, when the sample was treated successively and manually at 25 V, as rapidly as possible, the initial peak currents were: 106, 50, 36, 30, 22.5 and 22 mA corresponding to resistance of 231, 500, 694, 833, 1111 and 1136Ω respectively. When 1 min was allowed to elapse between successive treatments the initial currents recorded were: 106, 100, 90, 84, 78 and 74 mA.

The total amount of electricity Σq supplied to the sample at various times during the electrolysis was found by calculating the area under the I versus t curve using the trapezium rule. The

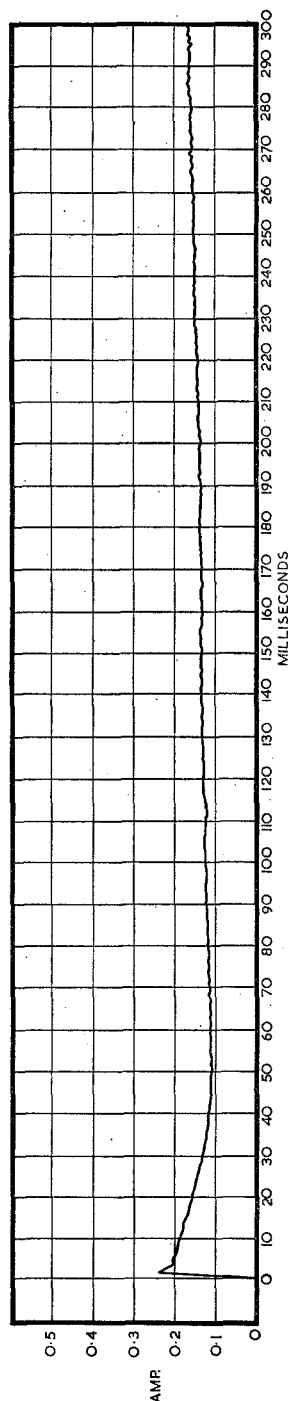


Fig. 8. Current-time trace at 175 V. Speed 2 m s^{-1} .

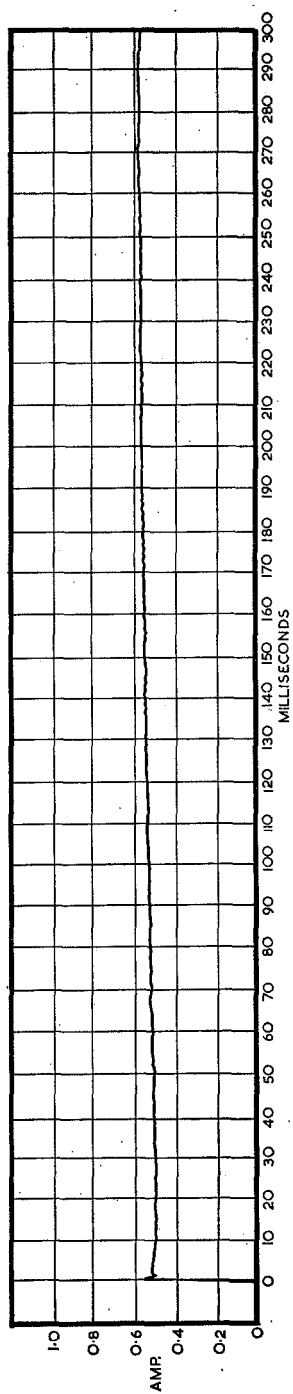


Fig. 9. Current-time trace at 250 V. Speed 2 ms⁻¹.

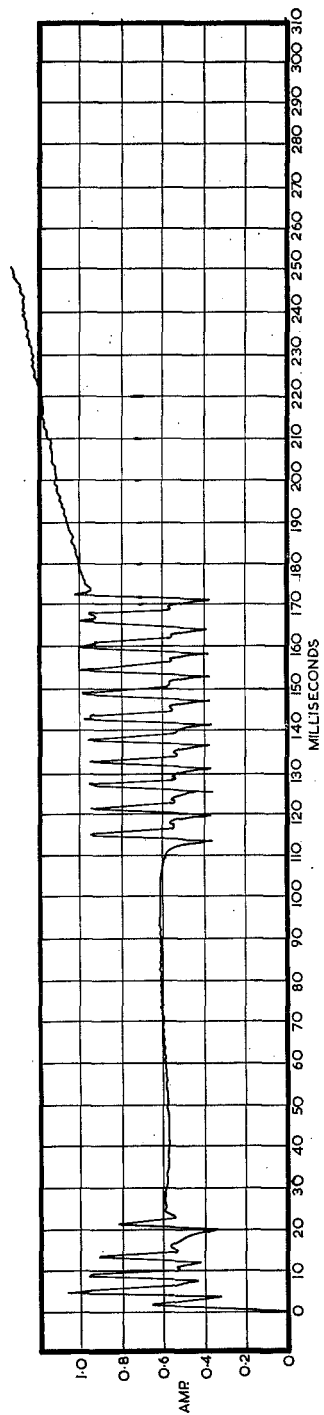


Fig. 10. Current-time trace at 300 V. Speed 2 m s⁻¹.

quantity of electricity passed at any particular time depends upon the applied voltage in the manner shown in Fig. 11 where Σq is plotted against V at three separate times of 100, 200 and 300 ms. In every case the charge passed is directly proportional to the voltage.

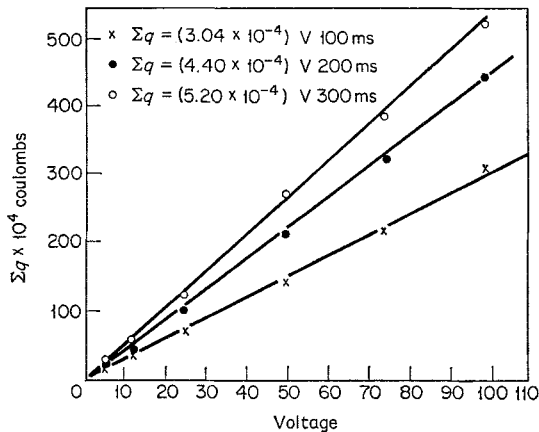


Fig. 11. Graph of charge against voltage at various times.

In view of this correlation, it is interesting to calculate the time taken to pass the same amount of charge into the glass at different voltages. A convenient quantity for comparison was 0.005 C and the graph of the reciprocal of the time to supply this amount of charge against the voltage is shown in Fig. 12. The linear part of the curve obeys the relation:

$$(0.79 \text{ V} - 5.5)t = 1 \quad (2)$$

Similar plots were made for 0.001 C and 0.02 C and although these curves do not apply over a

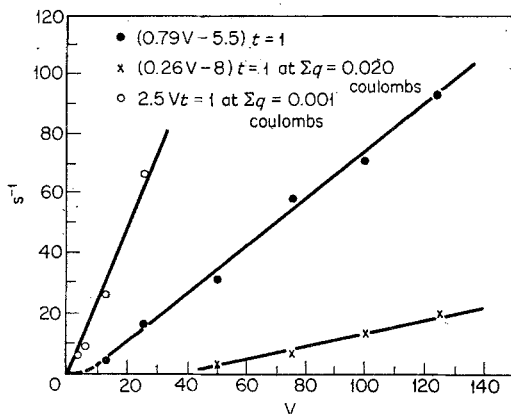


Fig. 12. Graph of reciprocal of time to supply 0.001, 0.005 and 0.020 C against voltage.

large range of voltage the linear parts may be expressed by the equations given in Fig. 12.

The size of the power inputs is rather surprising. In Fig. 13 the values calculated from the instantaneous values of the current at 100, 200 and 300 ms are plotted against the voltage. At 100 V the power inputs are 19, 11 and 7 W respectively. As would be expected, the power is proportional to the square of the voltage and the graphs are represented by the equations given.

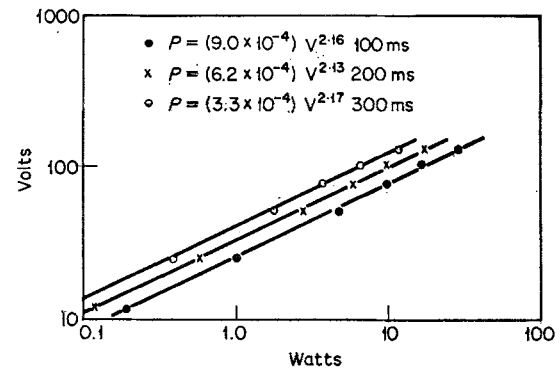


Fig. 13. Graph of input power against voltage at various times.

When the applied voltage from the power pack is removed, the voltage across the cell on open circuit drops rapidly. Figs. 14a and b are oscillograms of the voltage decay using microsecond and millisecond time bases with an initial applied voltage of 25 V. In the former the voltage falls almost linearly with time but in the millisecond range the decay levels off as shown.

The results for the various voltages in the microsecond, milliseconds, seconds and minutes ranges are given in Table 3. The most marked contrast occurs between the gradient constants in column 2, for the milliseconds and seconds regions. In the former they vary a hundred-fold in the interval from 125 V to 5 V but in the latter they are roughly constant. This is not surprising because the rate of decay in the millisecond region is dependent upon the initial applied voltage while by the time 10 s have elapsed (the start of measurement in the seconds range) the voltage is always approximately the same no matter what the size of the initial voltage.

These experiments were performed after a polarization of approximately 2 s but similar tests were carried out leaving the polarizing

Table 3. Voltage decay with time at 600°C.

Voltage	n	b	Equation	Range
Microsecond range. $V = V_0 - bt^n$				
100	0.92	2.5×10^4	$V = V_0 - (2.5 \times 10^4)t^{0.92}$	40–80 μ s
50	0.85	5.6×10^3	$V = V_0 - (5.6 \times 10^3)t^{0.85}$	30–600 μ s
25	0.84	2.3×10^3	$V = V_0 - (2.3 \times 10^3)t^{0.84}$	10–1000 μ s
5	0.98	5.6×10^1	$V = V_0 - (5.6 \times 10^1)t^{0.98}$	20–400 μ s
Millisecond range. $\exp \frac{2.3}{n} = bt$				
100	-52	86	$e^{-0.044} v = 86t$	1–10 ms
50	-23	49	$e^{-0.100} v = 49t$	0.3–10 ms
25	-11	33	$e^{-0.208} v = 33t$	0.2–10 ms
5	-0.61	0.00049	$e^{-3.78} v = 0.00049$	0.1–20 ms
Second range. $\exp \frac{2.3}{n} = bt$				
100	-0.30	1.0×10^{-10}	$e^{-7.6} v = (1.0 \times 10^{-10})t$	10–300 sec
50	-0.38	1.1×10^{-8}	$e^{-6.1} v = (1.1 \times 10^{-8})t$	5–300 sec
25	-0.41	2.0×10^{-7}	$e^{-5.6} v = (2.0 \times 10^{-7})t$	10–300 sec
5	-0.84	1.7×10^{-4}	$e^{-2.8} v = (1.7 \times 10^{-4})t$	10–200 sec
Minute range. $V = bt^n$				
100	-0.57	31	$V = 31t^{-0.57}$	2–15 min
50	-0.48	40	$V = 40t^{-0.48}$	10–100 min
25	-0.45	58	$V = 11t^{-0.35}$	6–90 min
5	-0.26	2.5	$V = 2.5t^{-0.26}$	1–5 min
Second range. Initial polarization 20 sec. $\exp \frac{2.3}{n} = bt$				
100	-0.34	9.6×10^{-11}	$e^{-6.8} v = (9.6 \times 10^{-11})t$	10–300 sec
50	-0.41	3.6×10^{-9}	$e^{-5.6} v = (3.6 \times 10^{-9})t$	10–300 sec
25	-0.45	2.1×10^{-8}	$e^{-5.1} v = (2.1 \times 10^{-8})t$	10–300 sec

V in volts; t in seconds.

voltage on for 20 s before breaking the circuit. The results in Table 3 show that the gradients are again roughly constant in the seconds range and similar to those measured after a polarization of 2 s.

Discussion

(a) Space charge

When a voltage is applied across the glass the current rises rapidly at first and then falls as shown in Fig. 3. At 25 V the variation of current with time is given by the expression (Table 2):

$$(190t + 7)I = 1 \quad (1)$$

The Zachariassen [3] model of glass structure postulates a random silica network with mobile, interstitial sodium ions and it is assumed in the present case that on the application of the voltage only these interstitial sodium ions move. There will then be developed in the glass a region near the anode short of sodium ions, i.e., having a negative charge. This charge, due to the stationary silica network, will tend to attract the sodium ions back in opposition to the applied field. It will build up with time as more and more interstitial sites are vacated until it is almost equal to the applied voltage; there will then be

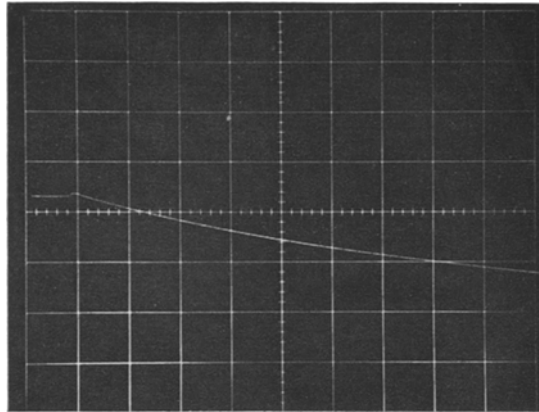
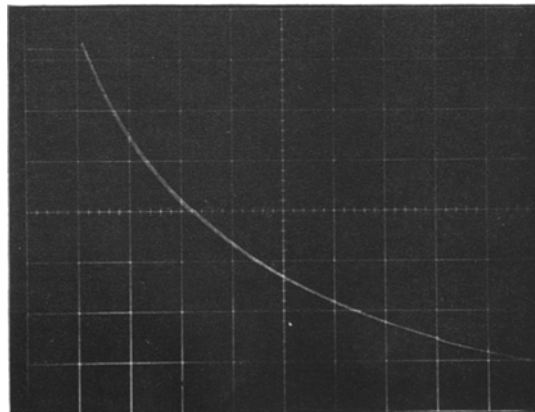


Fig. 14. Oscillograms of voltage decay against time
Initial voltage 25 V.
(a) Time base 100 $\mu\text{s}/\text{cm}$.



(b) Time base 1 ms/cm .

virtually no driving force on the sodium ions.

This will be true provided that lead ions from the anode pool do not replace the migrating sodium ions completely. Some replacement can be expected and indeed lead has been detected in trace amounts in the surface layers by X-ray fluorescence spectroscopy. Nevertheless the replacement is probably limited in view of the lower mobility of the lead ions, they being doubly charged and of larger ionic radius than the sodium ions (1.2 & 0.97 Å respectively). Furthermore, Isard and his collaborators [4] have shown, using the Tubandt method, that the current is carried almost completely by the sodium ions in sodium, lead silicate glasses containing 15% and more Na₂O. Even at 13% Na₂O the transport number of the sodium ion was approximately 0.95.

It is possible to calculate the diffusion coefficient of the sodium ion from the ionic conductivity using the Nernst-Einstein equation:

$$D_{\text{calc}} = \frac{\sigma_{\text{Na}} k t}{N e^2} \quad (3)$$

Here, σ_{Na} is the ionic conductivity of the mobile sodium ion, N the number of such ions and e the electronic charge. Taking the value of the initial current at 25 V as 127 mA the conductivity calculated from this is 1.3×10^{-3} mhos, cm⁻¹ resulting in a value of D_{calc} of 7.10×10^{-8} cm² s⁻¹. This may be compared with the figure of 5.44×10^{-8} cm² s⁻¹ obtained from the work of Haven and Verkerk [5] by extrapolation of their data for radioactive ²⁴Na diffusion at temperatures from 473 to 600°C in sodium silicate glass.

By dividing the measured by the calculated value of the diffusion coefficient the correlation factor, f , is obtained: it is 0.77 in the present case. This factor is a consequence of the non-random distribution of successive jumps of the sodium. The sodium ions may either move by a jump into a vacancy as it travels through the lattice (vacancy mechanism) or the interstitial sodium may jump on to a lattice site pushing the occupying sodium on to another interstitial site (interstitial mechanism).

For a lattice with 3-3 coordination (cf. [5]) the calculated values of f are 0.67 and 0.44 for the vacancy and interstitial mechanisms,

respectively. For a lattice with mixed 3-3 and 3-2 coordination the values are 0.33 and 0.35, respectively. The vacancy mechanism with 3-3 coordination is thus the most probable at 600°C.

However, Haven and Verkerk [5] found experimental values of f of from 0.49 to 0.52 at temperatures from 384 to 473°C. This suggests that the interstitial mechanism is operative at these lower temperatures.

Support for the idea of a space charge is provided by the work of Sutton [6] who has clearly demonstrated the presence of space charge in electrolysed soda lime glass. He applied electric fields using platinum blocking electrodes and measured the voltage at aluminium probes embedded in the glass at various distances from the anode and cathode. A typical result obtained at 410°C is given in Fig. 15.

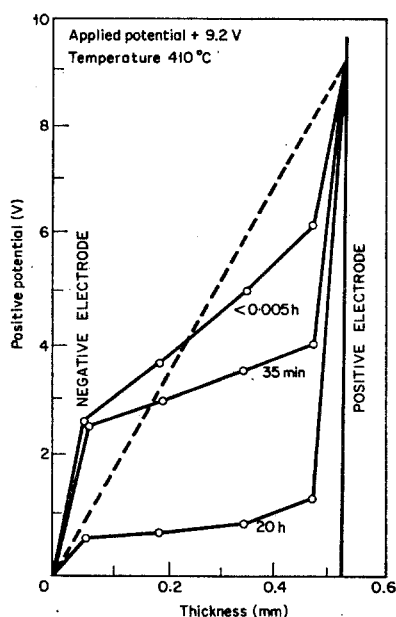


Fig. 15. Development of space-charge distribution at 410°C (after Sutton).

A characteristic of space charge phenomena is their persistence after long periods of time and the present process is no exception. Voltages of 0.5 V or so were measured on the digital voltmeter on samples that had been treated once and left overnight. The oscilloscope trace was opposite in direction to the decay curves obtained immediately on breaking the circuit. This suggests that a current was being driven through

the glass in the opposite direction due to some residual polarization remaining in the glass for long periods. The equation obeyed was:

$$e^{3.5V} = 71t \quad (4)$$

Even when the sample was short-circuited for 5 mins the behaviour was repeated giving a curve expressed by:

$$e^{4.6V} = 50t \quad (5)$$

Finally, it was found that approximately 0.3 V had to be applied in the reverse direction to an electrolysed sample to bring the oscilloscope spot back to the zero voltage position.

The shape of the oscillographic decay curves (Fig. 14) suggests the presence of a space charge or electrical double layer. Thus removal of the electric charge from the electrodes on breaking the circuit will be determined by the time constant of the oscilloscope. Taking the resistance and capacitance of the instrument as 1 M Ω and 10 pF, respectively, the time constant is 10 μ s. The fact that the voltage decays appreciably only after a period of milliseconds suggests that the decay is governed by the electrical properties of the glass. It is possible, using the voltage decay equations in Table 3, to calculate the current flowing during the discharge and the quantity of electricity passed. This is done by applying Ohm's law, taking the resistance of the oscilloscope and digital voltmeter as 1 M Ω , and integrating the resultant equation for the quantity of electricity supplied. The results of these calculations are for 25 V applied 2.39×10^{-8} C for the first millisecond, 1.38×10^{-5} C for the first 10 ms, 0.00068 C for 300s and 0.0037 C for 1½ h. The measured quantity of electricity supplied during a 300 ms electrolysis is more than this, being 0.0135 C as calculated from Fig. 3 by integrating using the trapezium rule.

It is probable that after the applied voltage has been removed not all the mobile sodium ions will return to the anodic layer. This is suggested by the increasing gradients of the I versus t graphs in Fig. 5 for samples treated at hourly intervals.

The system from 2.5 to 100 V where $1/I$ is proportional to t may be considered from the electrical point of view as a capacitance due to the double layer in series with a resistance due to

the base glass. When a voltage V is applied a large current will flow equal to V/R , where R is the a.c. resistance (270 Ω) of the base glass. This will decay exponentially, however, as the capacitance charges up, the current through the capacitance (and resistance) being given at any time t by the equation:

$$I = \frac{V}{R} \cdot e^{-t/RC} \quad (6)$$

The values of R and C may be taken as 270 Ω , the a.c. resistance of the bulk glass and 520 μ F, the capacity found from the gradient of the $\Sigma q/v$ curve, Fig. 11, at 300 ms. Substituting these values in equation (6) we have at 25 V:

$$I = 0.093e^{-7t} \quad (7)$$

The values of I calculated from this equation at various times are compared in Table 4 with the currents found experimentally. The agreement between the two sets of values is good and argues that the explanation given above is correct.

The exponential equation (6) may be expanded to give an equation of similar form to that found experimentally. Neglecting terms with powers of t greater than one we have:

$$I = \frac{V}{R(1+t/RC)} \quad (\text{for } t/RC \ll 1) \quad (8)$$

Rearranging,

$$I(t/VC + R/V) = 1 \quad (9)$$

which is similar in form to the experimental equation

$$I(190t + 7) = 1 \quad (1)$$

and predicts correctly that the coefficient of t and

Table 4. Experimental and calculated currents 600°C, 25 V.

Time (ms)	Current (mA) Experimental	Current (mA) $I = 0.093e^{-7t}$	Current (mA) $I(7t+1) = 0.093$
25	84	78	79
50	61	66	69
75	47	55	61
100	40	46	55
150	29	33	45
200	22	23	39
250	18	16	34
300	16	11	30

the constant term should both decrease with increasing voltage (cf. Table 2). Also at short times t when $t/RC \ll 1$ the calculated currents agree well with the experimental values (Table 4). However, at longer times, when $t/RC \ll 1$ and the exponential is not adequately expressed by two terms of the series expansion, the agreement breaks down.

(b) Surface conductivity

J. A. Yates (unpublished work) has developed an expression for the variation of current with time based solely on the change in resistance of the glass near the anode. It has been found to hold in the low voltage region where $1/I^2$ is proportion to t . He assumes that during electrolysis the glass consists of two regions, the bulk glass and a thin layer near the anode of lower specific conductivity, σ_x , in which all the mobile sodium ions have been replaced by lead ions from the anode. The treatment is based on three assumptions:

(i) the current at any time may be expressed in terms of the specific conductivity of the treated layer:

$$I = \sigma_x \cdot \frac{V_x}{y} \quad (10)$$

where V_x is the voltage drop across the layer of thickness y

(ii) the current may also be expressed in terms of the specific conductivity of the base glass:

$$I = \sigma_{Na} \cdot \frac{V - V_x}{l - y} \doteq \sigma_{Na} \cdot \frac{V - V_x}{l} \quad (11)$$

since the sample thickness $l \gg y$.

(iii) The rate of penetration of anode material is proportional to the rate of entry of the material and therefore to the current.

$$\frac{dy}{dt} = \frac{I}{Fc} \quad (12)$$

where c is the concentration of replaceable ions in g ion/cm³ and F is the Faraday constant. Taking these equations and eliminating y and V_x he arrives at the equation:

$$I = \left[\frac{\frac{1}{2} V \sigma_x Fc}{t + \frac{\sigma_x Fc l^2}{2\sigma_{Na}^2 V}} \right] \quad (13)$$

The equation predicts that I^2 should be inversely proportional to t and this is borne out in the present work at low voltages. At 1.0 V and 0.5 V the equations obeyed are:

$$I^2 10^4 (600t + 10) = 1 \quad (14)$$

$$I^2 10^5 (850t + 8) = 1 \quad (15)$$

The coefficients of t and the constant terms in the theoretical and experimental equations may be compared. Re-arranging equation (13) we have:

$$I_2 \left[\frac{2t}{V \sigma_x Fc} + \frac{l^2}{\sigma_{Na}^2 V^2} \right] = 1 \quad (16)$$

and taking the a.c. resistance at 1,000 Hz as 270 Ω .

$$\sigma_{Na} = \frac{0.4}{1.54 \times 270} = 9.7 \times 10^{-4} \text{ mhos cm}^{-1}$$

Substituting, the constant term in equation (16) works out at 1.7×10^5 and 6.8×10^5 at 1.0 V and 0.5 V, respectively, and these may be compared with the experimental values of 1×10^5 and 8×10^5 from equations (14) and (15) above.

Equations (14) and (16) can also be used to calculate a value of σ_x . Comparing co-efficients of t we have at 1 V:

$$\frac{2}{V \sigma_x Fc} = 600 \times 10^4$$

or

$$\sigma_x = 5.8 \times 10^{-10} \text{ mhos cm}^{-1}$$

The value calculated at 0.5 V was 8.1×10^{-11} mhos cm⁻¹.

The data of Strausse *et al.* [7] on lead silicate glass, PbO . SiO₂, were extrapolated from 400 to 600°C using the Rasch-Hinrichsen law to give a specific conductivity at 600°C of 3×10^{-6} mhos cm⁻¹; this is much larger than the values calculated above. Indeed the extrapolated specific conductivity for silica glass of 1×10^{-7} mhos cm⁻¹ at 600°C from the same paper is nearer than that for the lead silicate glass. Furthermore, Owen and Douglas [8] measured the specific conductivity of two samples of silica glass, one containing 0.04 ppm of sodium prepared by thermal decomposition of SiCl₄, and the other with 5 ppm of sodium prepared by the electrical fusion of quartz. The values at 600°C were 1×10^{-9} and 3×10^{-8} mhos cm⁻¹ respectively.

It would seem that the resistivity of the surface

layer, while different from that of the bulk glass, might correspond more closely to that of silica glass than to lead silicate glass and that the lead ions shown to be present in trace amounts by X-ray fluorescence spectroscopy might be relatively immobile in the silica network. Further work on this aspect will be carried out at higher temperatures. Whatever the nature of the surface the theory is fairly satisfactory in explaining the shape of the current-time graphs at low voltages. At voltages greater than 1 V, however, the current is inversely proportional to the time and not to the square root as predicted and the theory breaks down.

(c) Surface temperature

The sizes of the power inputs shown in Fig. 13 are surprising. At 100 V they are 20, 11 and 7 W at times of 100, 200 and 300 ms respectively. If a thin double layer is formed at the surface then most of the voltage will be dropped across this a few milliseconds after the voltage has been applied. It was decided to calculate the change in surface temperature with time. The following assumptions were made:

(1) The temperature rise in the glass is due to the electric current which is all converted to heat; there are no heat losses.

(2) The resistance of an infinitely thin surface film (whether due to lack of mobile charge carriers or to an electrical double layer) is much greater than the bulk glass; the heat may be assumed to be liberated at the surface.

The equations governing the surface temperature changes when the glass is subjected to a surface heat load which is a function of time are:

$$\alpha \frac{\partial^2 T}{\partial x^2} = \frac{\partial T}{\partial t} \quad (17)$$

and

$$\zeta = -K \frac{\partial T}{\partial x} \Big|_{x=0} \quad (18)$$

where σ = thermal capacity = 0.274 cal./°C [9]

ρ = density = 2.5 g . cm⁻³ [10]

K = thermal conductivity = 2.5 × 10⁻³ cal . cm⁻¹/°C [11]

α = thermal diffusivity = $K/\sigma\rho$ cm² g .⁻¹

ζ = heat load/unit area = 0.238 VI cal/cm⁻²

These equations were solved using the method of Laplace transformation resulting in the expression:

$$*T = \frac{0.238 V \sqrt{\alpha}}{\Gamma(3/2)K} \left[at^{\frac{3}{2}} + \frac{bt^{3/2}}{3/2} + \frac{2! Ct^{5/2}}{5/2 \cdot 3/2} + \frac{3! dt^{7/2}}{7/2 \cdot 5/2 \cdot 3/2} + \dots \right] \quad (19)$$

for the change of surface temperature with time when the experimental data obtained from the current-time curves were subjected to a polynomial fit of the form:

$$I = a + bt + ct^2 + dk^3 + et^4 + ft^5 + \dots \quad (20)$$

In Table 5 the results are tabulated at various voltages.

Table 5. Calculated surface temperature rise with time at various voltages

Time (ms)	25 V	100 V	150 V	175 V
50	2.89	11.52	23.64	34.93
100	2.96	11.80	30.53	46.69
150	2.88	11.48	35.73	57.80
200	2.79	11.13	39.16	68.52
250	2.70	10.77	42.48	79.28
300	2.62	10.43	45.77	90.43

At the lower voltages the surface temperature decreases continuously with time after a slight initial rise; it steadily increases at the higher voltages. It is thought that the heat causing this steadily increasing rise in surface temperature tends to disrupt the electrical double layer. This might be the case at 175 V (Fig. 8) for instance when an initial decay in current due to polarization is followed by a levelling out at a high value followed by a slow steady increase. Eventually, at 250 V, the double layer will be broken down very rapidly and there will be no fall in the current after the initial rise (of Fig. 9). The heat will then be generated throughout the bulk of the glass and the rise in temperature corresponding to this may be calculated.

We have:

$$\text{Heat load/unit area} = M \cdot \sigma \cdot \Delta T$$

where ΔT = bulk glass temperature rise.

Then,

$$250 \times 0.6 \times 0.238 = 1.75 \times 0.274 \times \Delta T$$

$$\text{and } \Delta T = 58.4^\circ\text{C} \cdot \text{s}^{-1}$$

At 300 V the corresponding figure is $70.1 \text{ C} \cdot \text{s}^{-1}$ and it is probable that the generation of the large amount of heat corresponding to this temperature rise is the cause of the rapid break-away observed.

While the absence of any decrease in current with time at 250 V implies that the heat is liberated throughout the bulk of the glass, it is nevertheless interesting to calculate the temperature rise which would have occurred had all the heat been generated in a thin surface film of high resistance. This will show whether or not the calculated surface temperatures are unreasonably high. It is also possible to calculate the temperature profile through the glass under these conditions and the gradient of this will indicate if there is any appreciable temperature differential across any surface film which might cause breakdown.

The surface temperature rise under conditions of constant heat load such as obtain at 250 V is given by the expression:

$$T^* = \frac{2F_0}{K} \left(\frac{\alpha t}{\pi} \right)^{\frac{1}{2}} \quad (21)$$

where F_0 = heat load/unit area = $0.288 \text{ V} \times I$, and the other symbols have their usual meaning.

Substituting we have:

$$T^* = \frac{2 \times 23.1}{2.5 \times 10^{-3}} \sqrt{\frac{2.5 \times 10^{-3} \cdot t^{\frac{1}{2}}}{2.5 \times 0.274\pi}} \quad (22)$$

$$T^* = 630t^{\frac{1}{2}} \quad (23)$$

In Fig. 16, T^* is plotted against t . It is clear that after 100, 300 and 1000 ms the surface temperature rise is 200, 350 and 630°C giving an actual surface temperature at these times of 800, 950 and 1230°C , respectively. These temperatures seem excessively large for any thin surface layers to stand and it is thought that the former analysis of heat liberated throughout the bulk of the glass at this voltage is more realistic.

Any surface layers that may, however, be formed will not be broken down by a temperature differential across them. This is shown by calculating the temperature profile through the

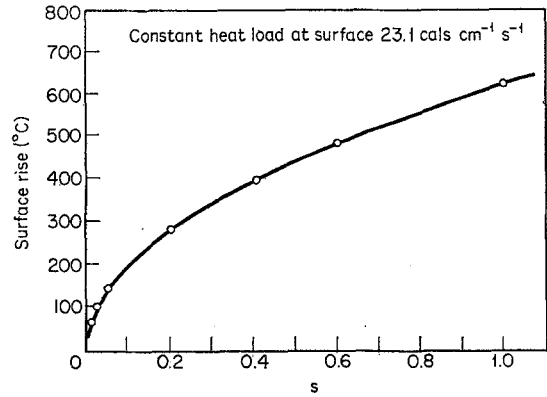


Fig. 16. Surface temperature rise against time at 250 V.

glass, again assuming that all the heat is liberated at the surface. It is given by the expression:

$$T_{(x,t)} = \frac{2F_0}{K} \left[\left(\frac{\alpha t}{\pi} \right)^{\frac{1}{2}} \cdot e^{-\frac{x^2}{4\alpha t}} - \frac{x}{2} \operatorname{erfc} \frac{x}{2\sqrt{\alpha t}} \right] \quad (24)$$

where x is the distance from the anode. Thus, for a surface temperature rise of 350°C which occurs in 300 ms at 250 V the temperature profile is that shown in Fig. 17. The profile is shallow and

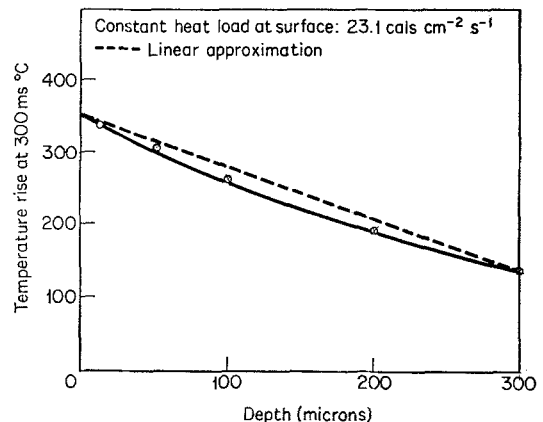


Fig. 17. Temperature rise at 300 ms against depth from anode at 250 V.

would not result in an appreciable temperature differential across a film of thickness $\sim 50 \mu$ (Sutton) or 52 \AA (Yates, equation 13).

Acknowledgments

Thanks are due to Mr H. Cole for encouraging the investigation; to Mr J. A. T. Jacquet, to Mr W. Hopwood and Mr R. Saunders for useful discussions on the electrical theories

involved; to Mr F. Roué for experimental assistance; to Dr K. Craine for help with the mathematical analysis of the thermal effect and the mathematic section for computer facilities; to Mr R. Hesford for contacts in the electronics field; to Mr D. Barnett of Data Acquisition and Measurement Research for supplying the delay and trigger unit. The author wishes to thank Messrs Pilkington Brothers and Dr D. S. Oliver, Director Group Research and Development for permission to publish this article.

References

- [1] E. Warburg, *Ann. Physik. Chem.* **21** (1884) 622.
- [2] F. Tegetmeier, *Ann. Physik. Chem.* **41** (1890) 18.
- [3] W. H. Zachariassen, *J. Amer. Ceram. Soc.* **54** (1932) 3841.
- [4] K. Hughes, J. O. Isard and G. C. Milnes, *Physics & Chemistry of Glasses*, **9** (1968) 43.
- [5] Y. Haven and B. Verkerk, *Physics & Chemistry of Glasses* **6** (1965) 38.
- [6] P. M. Sutton, *J. Amer. Ceram. Soc.* Pt. I **47** (1964) 188; Pt II *ibid.*, 219.
- [7] S. W. Strauss, D. G. Moore, W. N. Harrison and L. E. Richards. *J. Res. Natl. Bur. of Standards*, **56** (1956) 135.
- [8] A. E. Owen and R. W. Douglas, *Journ. Soc. Glass Tech.*, **43** (1959) 159T.
- [9] A. Hodgson LR132 July 1963. Fig. 6. Measurement of the Specific Heat of Glass at Elevated Temperatures.
- [10] D. R. Oakley, private communication.
- [11] H. S. Carslaw and J. C. Jaeger, 'Conduction of Heat in Solids', 2nd Ed, Oxford University Press.